

Обзор ArXiv/astro-ph, 15-20 октября 2021

От Сильченко О.К.

ArXiv: 2110.07935

Star-Forming S0 Galaxies in SDSS-IV MaNGA Survey

Ke Xu,^{1,2} Qiusheng Gu,^{1,2}★ Shiyong Lu,^{1,2} Xue Ge³ Mengyuan Xiao^{1,2} and Emanuele Contini^{1,2}

¹*School of Astronomy and Space Science, Nanjing University, Nanjing 210093, P. R. China*

²*Key Laboratory of Modern Astronomy and Astrophysics (Nanjing University), Ministry of Education, Nanjing 210093, China*

³*School of Physics and Electronic Engineering, Jiangsu Second Normal University, Nanjing, Jiangsu 211200, China*

Accepted XXX. Received YYY; in original form ZZZ

ABSTRACT

To investigate star-forming activities in early-type galaxies, we select a sample of 52 star-forming S0 galaxies (SFS0s) from the SDSS-IV MaNGA survey. We find that SFS0s have smaller stellar mass compared to normal S0s in MaNGA. After matching the stellar mass to select the control sample, we find that the mean Sérsic index of SFS0s' bulges (1.76 ± 0.21) is significantly smaller than that of the control sample (2.57 ± 0.20), suggesting the existence of a pseudo bulge in SFS0s. After introducing the environmental information, SFS0s show smaller spin parameters in the field than in groups, while the control sample has no obvious difference in different environments, which may suggest different dynamical processes in SFS0s. Furthermore, with derived N/O and O/H abundance ratios, SFS0s in the field show nitrogen enrichment, providing evidence for the accretion of metal-poor gas in the field environment. To study the star formation relation, we show that the slope of the spatially resolved star formation main sequence is nearly 1.0 with MaNGA IFU data, confirming the self-regulation of star formation activities at the kpc scales.

48+48: SF+non-SF S0, SDSS

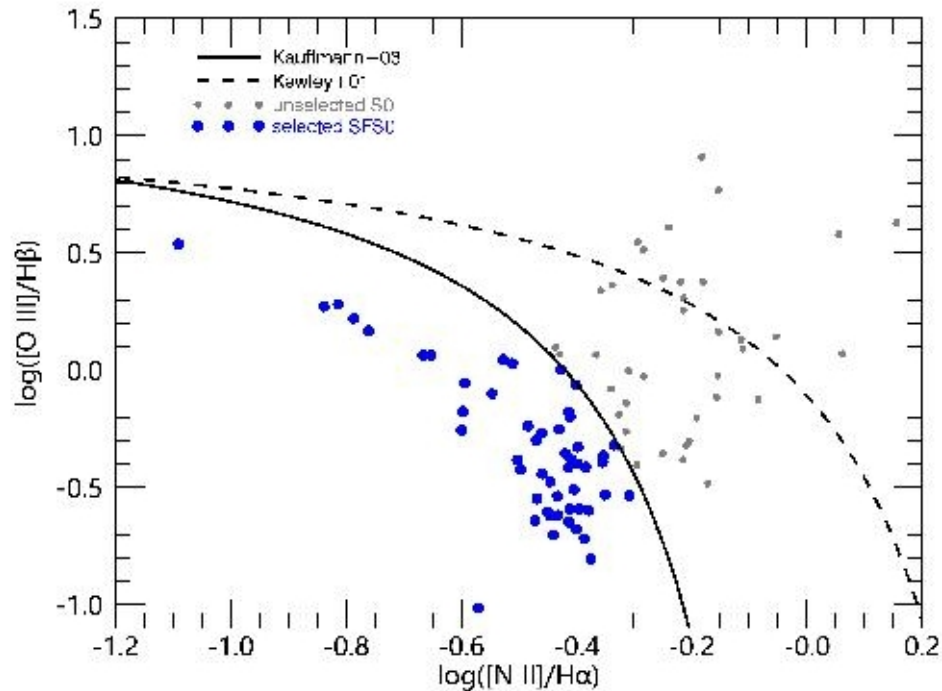


Figure 1. The BPT diagram for SFS0s. The blue (grey) dots are the selected SFS0s (unselected S0s). The solid and dashed demarcation lines are taken from Kewley et al. (2001) and Kauffmann et al. (2003b).

Хотя дальше данные MaNGA!

Sersic для балджей: вывод - у звездообразующих есть псевдобалджи

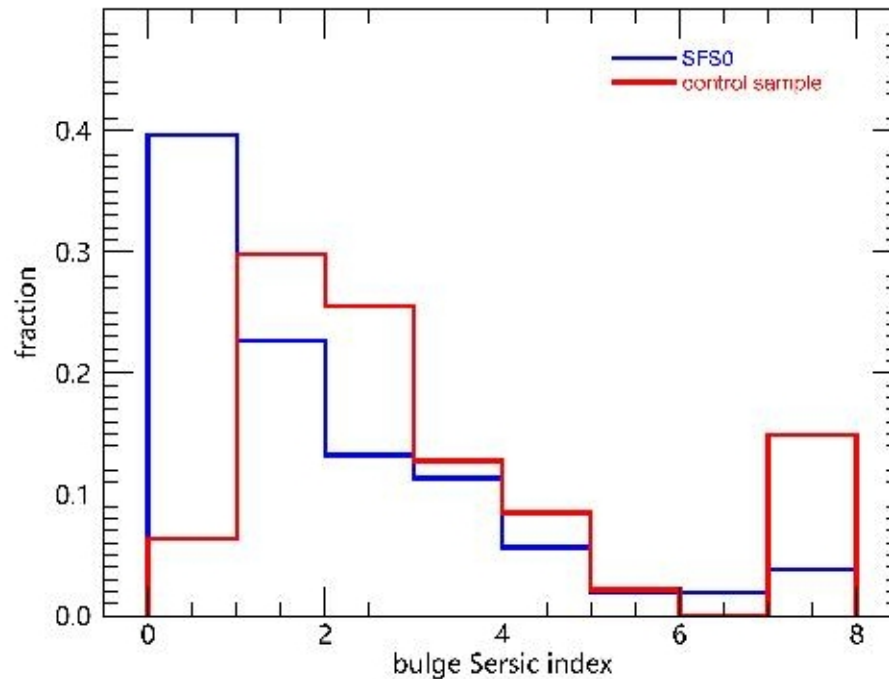


Figure 3. The distributions of the Sérsic index of bulges. Blue lines represent SFS0s, and red lines represent the control sample. The excess at $n=8$ is due to the upper limit in the morphological fitting.

Так все-таки: что там с главной последовательностью??

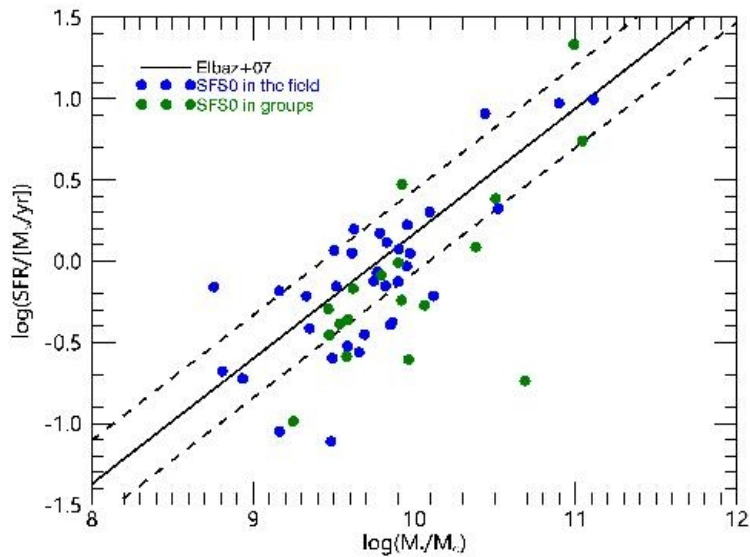


Figure 4. The star formation main sequence of SFSOs. The blue points are isolated SFSOs, and the green points are SFSOs groups. The solid line is from Elbaz et al. (2007), and the two dashed lines correspond to $\pm 1\sigma$ thresholds.

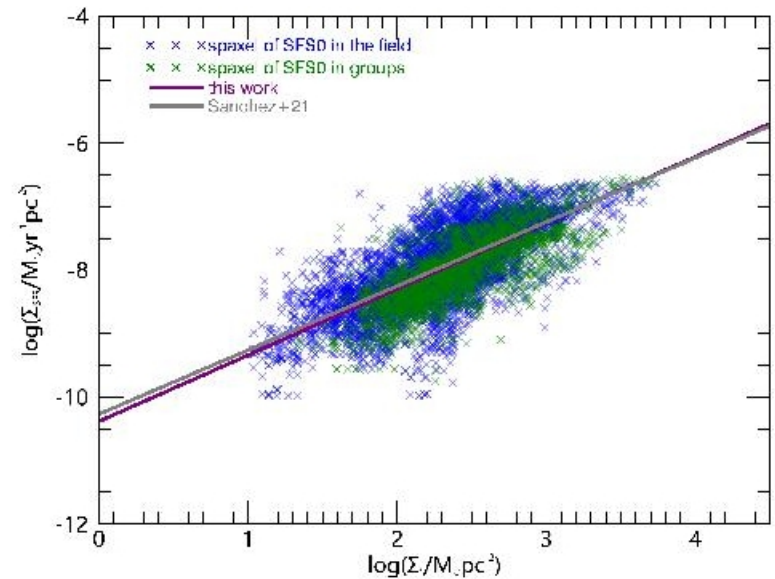


Figure 5. The spatially resolved SFMS for our SFSOs. Blue crosses: star-forming spaxels from SFSOs in the field. Green crosses: star-forming spaxels from SFSOs in groups. The solid purple line is the best-fitting of all the spaxels in this work, while the solid grey line is the fitting of the CALIFA dataset from Sánchez et al. (2021).

Наконец различие с окружением: В поле пониженный спин

$$\cos i = \sqrt{\frac{(1 - \epsilon)^2 - q_0^2}{1 - q_0^2}}, \quad (1)$$

where i is the inclination, ϵ is the ellipticity, and q_0 is the intrinsic axis ratio of edge-on galaxies, which is assumed to be 0.2 (Tully & Pierce 2000). We reconstruct the spatially resolved rotational velocity as in Deeley et al. (2020):

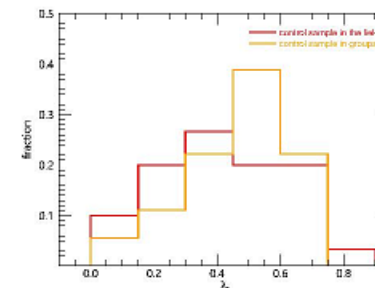
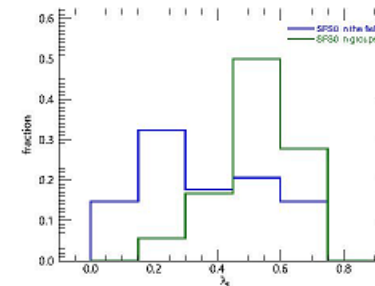
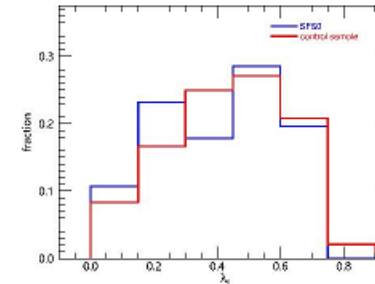
$$v_t = \frac{v_r}{\sin i \cos \theta}, \quad (2)$$

where θ is the azimuthal angle from the major axis, v_t and v_r are the rotational and radial velocities in each spaxel, respectively.

Following Cappellari et al. (2007), the spin parameter within $1.5 R_e$ is defined as:

$$\lambda_R = \frac{\sum_{n=1}^N F_n R_n |v_t|}{\sum_{n=1}^N F_n R_n \sqrt{v_t^2 + \sigma_n^2}}, \quad (3)$$

where n denotes the n th spaxel, F_n is the flux, R_n is the distance from the centre, and σ_n is velocity dispersion. The rotational velocity (v_t) is used to minimize the influence of inclination.



SF

non-SF

Figure 6. The distributions of spin parameters. The top panel: SFS0 and the control sample. The middle panel: the SFS0s in the field and in groups. The bottom panel: the control sample in the field and in groups.

Химия: избыток азота=аккреции металлобедного газа (?)

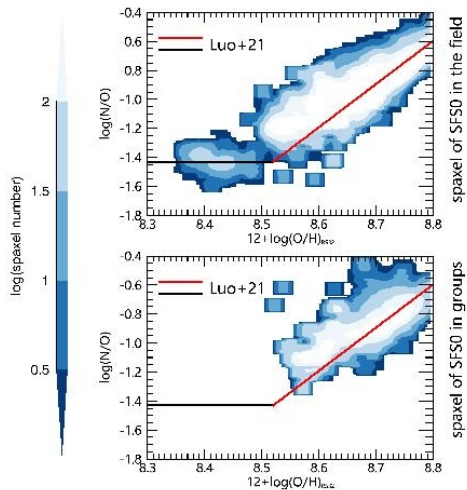


Figure 7. The N/O vs O/H plane for SFSOs. The upper and lower panels are the spaxels from SFSOs in the field and in groups individually. The black and red solid lines are the result from Luo et al. (2021). The color grid represents the spaxel number.

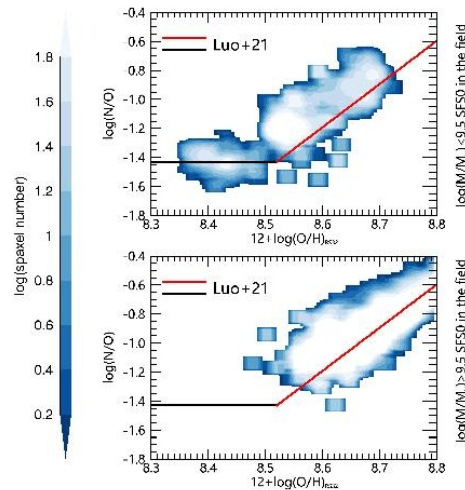


Figure 8. The N/O vs O/H plane for the spaxels from low-mass (upper) and high-mass (lower panel) SFSO in the field. The black and red are from Luo et al. (2021). The color grid represents the spaxel number.

metal-poor gas, they would locate above the relation between N/O and O/H, resulting in N/O abundance excess. During the transport of gas into galaxies, star formation is sustained.

Does it happen in SFSOs? We follow the same procedure to probe the corresponding properties and restrict the spaxel with $H\alpha$ equivalent length $> 6 \text{ \AA}$ and emission lines with $S/N > 5$ to calculate the metallicity. We adopt the relation in Loaiza-Agudelo et al. (2020) to calculate N/O:

$$\log(N/O) = 0.73 \times N2O2 - 0.58, \quad \text{and} \quad (8)$$

$$N2O2 = [NII]\lambda 6584 / [OII]\lambda\lambda 3727, 3729.$$

Instead of using the common O3N2 method in consideration of degeneracy, the O/H is obtained from the RS32 method in Curti et al. (2020), which is only mildly dependent on ionization parameter:

$$RS_{32} = \sum_N c_n [12 + \log(O/H) - 8.69]^n, \quad \text{and} \quad (9)$$

$$RS_{32} = [OIII]\lambda 5007 / H\beta + [SII]\lambda\lambda 6717, 31 / H\alpha,$$

where c_n is from Table 2 in Curti et al. (2020).

Ура! В массивных S0 – аккрецированные внешние кольца

